# Synthesis of Nanostructure Materials and their Application in Gas Sensing

A.V.Kadu[1]* & S. G. Ibrahim [2]
1)Department of Chemistry, Prof Ram Meghe College of Engineering & Management, Badnera- Amravati 444701, (M.S.) India.
2) Nanostructured Thin Film Laboratory, Department of Physics, Prof Ram Meghe College of Engineering & Management, Badnera- Amravati 444701, (M.S.) India.
*Email address: ashishkadu26@rediffmail.com*

***Abstract:-*** The $Sm_{0.9}Ce_{0.1}Fe_{1-x}La_xO_3$ ($0 \leq x \leq 0.10$) nanostructures have been synthesized and studied as the sensing element for the detection of $H_2S$. The nanostructured materials were synthesized by sol-gel method. The results of scanning electron microscopy and X-ray diffraction revealed that the grains of these materials are composed of nano-crystallites. The gas-sensing performance of the as-prepared $Sm_{0.9}Ce_{0.1}Fe_{0.95}La_{0.05}O_3$ nanoparticles was investigated towards different reducing gases like ammonia ($NH_3$), hydrogen sulfide ($H_2S$), Ethanol ($C_2H_5OH$) and liquefied petroleum gas (LPG).Gas sensing properties of $Sm_{0.9}Ce_{0.1}Fe_{0.95}La_{0.05}O_3$ nanostructure thick films were studied for low concentration $H_2S$ gas at $210^0$ C. The nanostructure synthesized material is a promising material for semiconductor gas sensor to detect poisonous gas like $H_2S$ at lower operating temperature with high sensitivity and selectivity.

***Keywords:*** *Gas sensor, Selectivity, Sensor response, Recovery*

*****

## 1. INTRODUCTION

Semiconductor metal oxides as gas sensing materials have been investigated widely for practical applications, such as gas leak detection and environmental monitoring. One of the most pomising approaches to the next generation of high performance gas sensors is the development of nanostructured sensing materials [1]. With the growing attention to environmental problems and the increase of the standard of living, there are imperative needs for solid-state gas sensors with high sensitivity and excellent selectivity in air quality monitoring and automotive application, especially for monitoring Hydrogen sulphide gas ($H_2S$).

However, relatively fewer studies concern the sensing characteristics towards $H_2S$, which is one of the noxious, colourless and aromatic gases [2,3]. Thus, there is a large need for making every attempt to investigate improved $H_2S$ gas sensors. As it is well known, the gas sensing mechanism in metal oxide materials is surface controlled, in which; the grain size, surface states and oxygen adsorption play an important role. Therefore, the morphology and surface-to-volume ratio of the material needed to be further optimized to improve gas-sensing properties. Presently, two practical approaches have been adopted to satisfy the above needs, namely, doping and modifying the material synthesis process.

Perovskites have a great potential for use as gas sensors because they have high electrical conductivity and are capable of catalytic activity involving oxidation–reduction reactions. The $ABO_3$ type perovskite oxides have been extensively used as gas sensors. The versatility of this $ABO_3$ type structure is that substitution at the A site and/or the B-site can be done to obtain desirable sensitivity and selectivity [4-9]. In the present study nanocrystalline films have been prepared by sol-gel technique. In particular, X-ray diffraction, Scanning electron microscopy observations, have been considered in order to determine both the micro-structure and gas sensing properties of $H_2S$ gas sensor.

## 2. EXPERIMENTAL TECHNIQUE

### 2.1. Material Synthesis

All the reagents used for the synthesis of $Sm_{0.9}Ce_{0.1}Fe_{1-x}La_xO_3$ ($0 \leq x \leq 0.10$) nanoparticles were analytical grade and used as received without further purification. The stoichiometric amounts of Samarium nitrate [$Sm(NO_3)_3 \cdot 6H_2O$], cerium nitrate [$Ce(NO_3)_3 \cdot 6H_2O$], ferric nitrate ($Fe(NO_3)_3.9H_2O$) and Lanthanium nitrates [$La(NO_3)_3.6H_2O$] were dissolved in deionized water under magnetic stirring. Then citric acid ($C_6H_8O_7.H_2O$) was mixed in the metal nitrate solution to chalet with metal ions in the solution. The molar ratio of citric acid to total moles of nitrates was maintained at 1:3. A small amount of ammonia was added drop-wise into the solution to adjust pH value to about 7 and stabilize the nitrate-citrate solution. The neutralities solution was evaporated to dryness by heating at $90^0$C on a hot plate with continuous stirring until it becomes viscous and finally formed a very viscous gel. The temperature is further raised up to $120^0$C so that the ignition of the gel starts. The dried gel burnt completely in a self propagating combustion manner to form a lose powder. Finally the as burnt powders were annealed at temperature $550^0$C for 6 hrs with a heating rate of $50^0$C per minute to obtain the Peroskite phase.

### 2.2. Structural & Gas Sensing Characterization

The synthesized samples were characterized for their structure by powder X-ray diffraction (XRD) using a Siemens D 5000 diffractometer. The XRD data were recorded by using Cu $K_\alpha$ radiation (1.5406 A°). The average crystallite size of the samples was estimated with the help of Scherrer's equation using the diffraction intensity of all prominent lines. The fine powder was observed under a JEOL, JSM – 5600 N scanning electron microscope (SEM) by dispersion it on a carbon paste to determine the morphology. A small constant voltage was applied across the sample and the current through the sample was measured with respect to temperature. Temperature of the sample in the form of pellet was measured with chromel-alumel thermocouple. The measuring principle of gas sensing properties is described elsewhere. The gas sensitivity (*S*) is defined as the ratio of the change of resistance in presence of gas ($R_g$) to that in air ($R_a$),

$$S = (R_a - R_g)/R_a = \Delta R/R_a$$

## 3. RESULTS AND DISCUSSIONS

### 3.1 X-ray Diffraction Study

The X-ray diffraction patterns of $Sm_{0.9}Ce_{0.1}FeO_3$ and $Sm_{0.9}Ce_{0.1}Fe_{0.95}La_{0.05}O_3$ are shown in Fig. 1. The comparison of these X-ray diffraction patterns shows that all these perovskites were single phase with orthorhombic structure. The comparison with standard JCPDS card # 39-1490 indicates an orthorhombic symmetry from the Pnma (62) space group [10]. No additional peaks were observed that would indicate a separate phase. From this data we conclude that a single perovskite phase is obtained for each material with particle size 40-50 nm. Peak positions and full-width-half-maxima were used to determine cell parameters and crystallite sizes for all the perovskites.

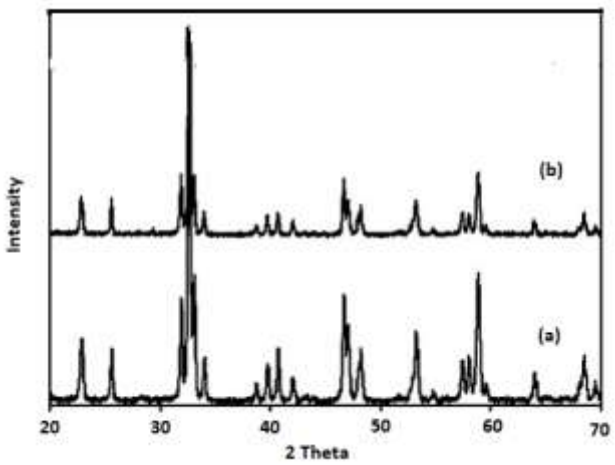


**Fig.1.XRD pattern of (a) $Sm_{0.9}Ce_{0.1}FeO_3$ & (b) $Sm_{0.9}Ce_{0.1}Fe_{0.95}La_{0.05}O_3$ calcined at 550 $^0$C**

### 3.2. Morphology study

The SEM technique was employed for finding morphology of $Sm_{0.9}Ce_{0.1}Fe_{0.95}La_{0.05}O_3$ as synthesized powder, calcined at 550$^0$ C. One can notice the presence of macro-agglomerations of very fine particles. The particle shapes are not well defined. Many large and small pores are present in the whole material. We assumed that the pores are mainly inter-granular because intra-granular pores are not seen on the SEM photograph.

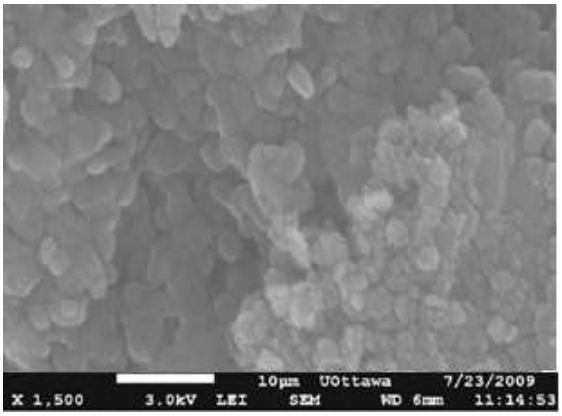


**Fig.2. SEM images of $Sm_{0.9}Ce_{0.1}Fe_{0.95}La_{0.05}O_3$, calcined at 550$^0$ C**

### 3.3. Gas-sensing characteristics

The gas-sensing responses of $Sm_{0.9}Ce_{0.1}FeO_3$ to different reducing gases like ammonia ($NH_3$), hydrogen sulfide ($H_2S$), Ethanol ($C_2H_5OH$), Hydrogen ($H_2$) and liquefied petroleum gas (LPG) as a function of operating temperature were studied. The $Sm_{0.95}Ce_{0.05}FeO_3$ nanocrystalline powder calcined at 550 $^0$C for 6h exhibits good response to $H_2S$ at 300$^0$C. The response of $Sm_{0.95}Ce_{0.05}FeO_3$ towards $NH_3$, $H_2S$, Ethanol, $H_2$ and LPG is depicted in Fig. 3. It was found that the sensor element based on $Sm_{0.95}Ce_{0.05}FeO_3$ could detect $H_2S$ at 300$^0$C with poor selectivity.

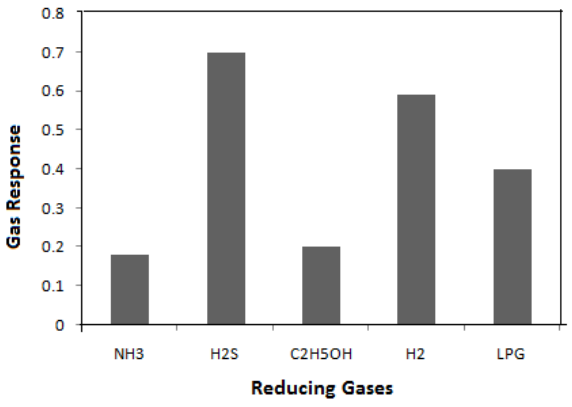


**Fig.3. Response of $Sm_{0.95}Ce_{0.05}FeO_3$ towards reducing gases at an operating temperature 300$^0$ C.**

The reducing gas R acting on the $Sm_{0.95}Ce_{0.05}FeO_3$ surface can be described as

$$R\ (gas) \leftrightarrow R\ (ads)$$
$$O_2^-\ (ads) + e^- \leftrightarrow 2O^-\ (ads)$$
$$R\ (ads) + O^-\ (ads) \leftrightarrow RO(ads) + e^-$$

In the absence of R, electrons are removed from $Sm_{0.95}Ce_{0.05}FeO_3$ conduction band by the reduction of $O_2$, resulting in the formation of $O^-$ species and consequently the resistance of $Sm_{0.95}Ce_{0.05}FeO_3$ sensor increases. When R is introduced, it reacts with $O^-$ (ads) to form RO, and electrons enter the conduction band of $Sm_{0.95}Ce_{0.05}FeO_3$ leading to decrease of resistance.

The reactions involved during the ethanol sensing are summarized below [11]:

$$H_2S + 3O^-ads \leftrightarrow SO_2 + H_2O + 3e^-$$

Fig. 4 illustrates the response of $Sm_{0.95}Ce_{0.05}FeO_3$ and $Sm_{0.9}Ce_{0.1}Fe_{0.95}La_{0.05}O_3$ as a function of the operating temperature towards 100 ppm $H_2S$ gas. From the plots it is clearly evident that the $Sm_{0.9}Ce_{0.1}Fe_{0.95}La_{0.05}O_3$, there was notable enhancement in the response to 100 ppm $H_2S$ gas with reduction in the optimal operating temperature. The operating temperature for maximum response towards 100 ppm $H_2S$ gas was observed at lower operating temperature 230 $^0$C.

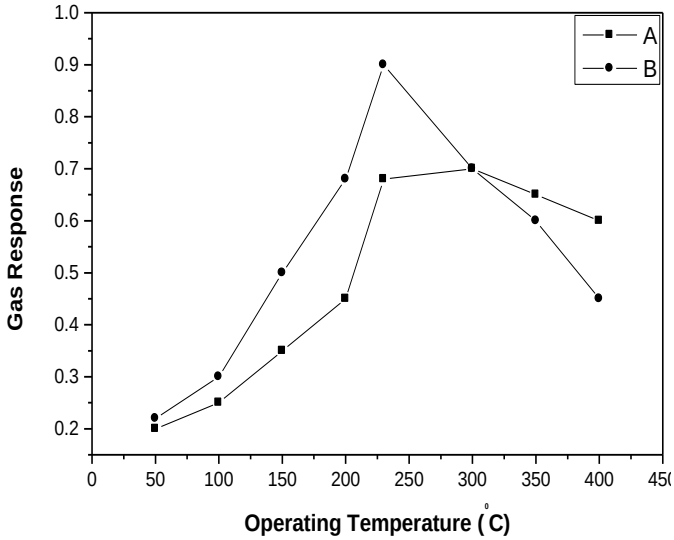


**Fig.4: Response of $Sm_{0.95}Ce_{0.05}FeO_3$ and $Sm_{0.9}Ce_{0.1}Fe_{0.95}La_{0.05}O_3$ towards 100 ppm $H_2S$ gas**

To know about the selective behavior of $Sm_{0.9}Ce_{0.1}Fe_{0.95}La_{0.05}O_3$ towards $H_2S$ gas at optimal operating temperature, its response to $NH_3$, Ethanol, $H_2$ and LPG was also studied. The results are shown in Fig. 5. Furthermore, the response of $Sm_{0.9}Ce_{0.1}Fe_{0.95}La_{0.05}O_3$) to $H_2S$ gas was also measured at 230 $^0$C in the presence of other tested interfering gases. For this, 100 ppm $H_2S$ gas was injected in the testing chamber, and then, in its presence, LPG, $NH_3$, $H_2$ and Ethanol were also injected. Thereafter, the change in the response of sensor element to 100ppm of $H_2S$ gas was measured.

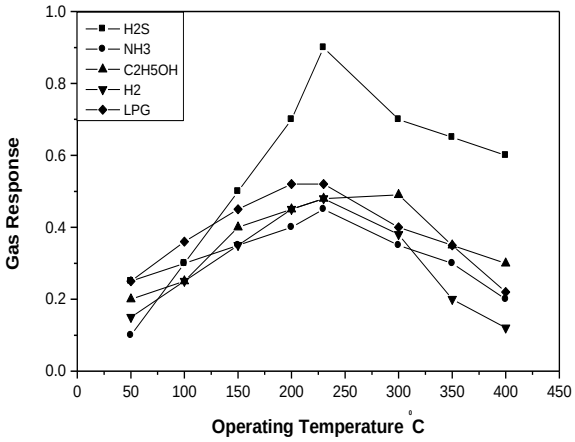


**Fig.5 : Selectivity of $Sm_{0.9}Ce_{0.1}Fe_{0.95}La_{0.05}O_3$ for different reducing gases.**

It can be seen that the response of sensor elements to $H_2S$ gas remains high after the introduction of interfering gases like LPG, $NH_3$ and Ethanol besides $H_2S$ gas in the testing chamber. The influence of other reducing gases that are additionally present on the $H_2S$ gas characteristics was found to be nearly 0–14% at 230 $^0$C. So, it can be seen that $Sm_{0.9}Ce_{0.1}Fe_{0.95}La_{0.05}O_3$ increases the response along with enhancing the selectivity to $H_2S$ gas.

The response-recovery characteristics of the $Sm_{0.95}Ce_{0.05}FeO_3$ and $Sm_{0.95}Ce_{0.05}Fe_{0.95}La_{0.05}O_3$ sensor elements to 100ppm H2S gas at 230$^0$ C are shown in Fig. 7. The response and recovery time of the $Sm_{0.95}Ce_{0.05}Fe_{0.95}La_{0.05}O_3$ was found to reduce as compared with unmodified $Sm_{0.95}Ce_{0.05}FeO_3$. The result indicates that the $Sm_{0.95}Ce_{0.05}Fe_{0.95}La_{0.05}O_3$ sensor can meet the practical application for $H_2S$ gas detection.

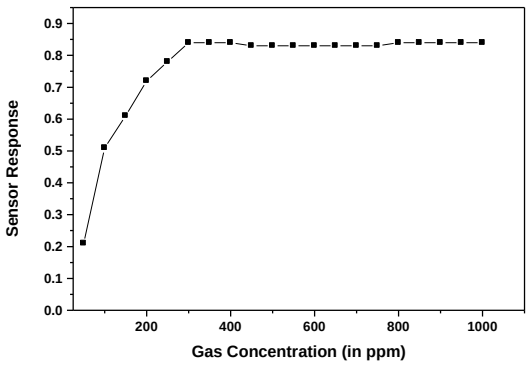


**Fig.6: Variation of Gas sensitivity with gas concentration**

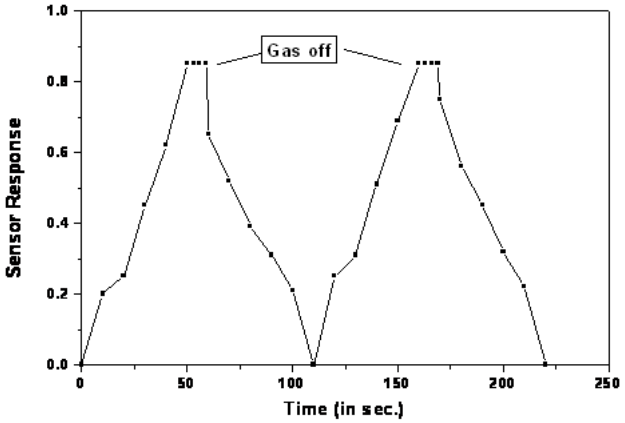


**Fig.7. Response and recovery time of $Sm_{0.9}Ce_{0.1}Fe_{0.95}La_{0.05}O_3$ for $H_2S$ gas.**

## 4. CONCLUSIONS

The perovskite $Sm_{0.9}Ce_{0.1}Fe_{1-x}La_xO_3$ were successfully synthesized by citrate sol-gel method followed by calcinations at $550^0$C. X-ray diffraction patterns shows that all these perovskites were single phase with orthorhombic structure with particle size 40-50 nm. The SEM image shows that the presence of macro-agglomerations of very fine particles. The particle shapes are not well defined. Many large and small pores are present in the whole material. $Sm_{0.9}Ce_{0.1}Fe_{0.95}La_{0.05}O_3$ sensor exhibited good selectivity to $H_2S$ gas at an operating temperature 230 $^0$C. This means that $Sm_{0.9}Ce_{0.1}Fe_{0.95}La_{0.05}O_3$ sensor can be a good candidate for practical use in detecting $H_2S$ gas because of the good characteristics mentioned.

## References

[1] O.K. Tan,W. Cao,Y. Hu,W. Zhu, Ceram. Int. 30 (2004) 1127–1133.
[2] A.B. Bodade, A.M. Bende, G.N. Chaudhari, Vacuum 82 (2008) 588-564.
[3] S.S. Badadhe, I.S. Mulla, , Sensors and Actuators B 143 (2009) 164-170.
[4] X. Liu, J. Hu, B. Cheng, H. Qin, M. Jiang, Current Applied Physics 9 (2009) 613–617.
[5] L. Chen, J. Hu, S. Fang, Z. Han, M. Zhao, ZhanleiWu, X. Liu, H. Qin, Sensors and Actuators B 139 (2009) 407–410.
[6] G.N. Chaudharia, N.N. Gedam, S.V. Jagtap, S.V. Manorama, Talanta 77 (2009) 1675–1679.
[7] S.M. Bukhari, J.B. Giorgi, The Journal of the Electrochemical Society 158 (2011) 1027-1033.
[8] S.M. Bukhari, J.B. Giorgi, Solid State Ionics 180 (2009) 198–204.
[9] J. Zosel, D. Franke, K. Ahlborn, F. Gerlach, V. Vashook, U. Guth, Solid State Ionics 179 (2008) 1628–1631.
[10] S.M. Bukhari, J.B. Giorgi, Sensors and Actuators B 155 (2011) 524–537.
[11] Vishal Balouriaa,b, Arvind Kumara, S. Samantaa, A. Singha, Mahajan, R.K. Bedib, D.K. Aswala, S.K. Gupta, Sensors and Actuators B 181 (2013) 471– 478

.